Available online at www.sciencedirect.com
SCIENCE DIRECT
Journal of Organometallic Chemistry 691 (2006) 1693–1702
Journal of Organometallic Chemistry
www.elsevier.com/locate/jorganchem

Chiral self-assembly of methyltin(IV)-naproxenates: Combining dative Sn–O bonds, secondary Sn···O interactions and C–H···O hydrogen bonding to make an inter-helical meander-shaped network and a cross-linked Z-shaped ribbon

Andrea Deák *, Gábor Tárkányi

Institute of Structural Chemistry, Chemical Research Center, Hungarian Academy of Sciences, Pusztaszeri út 59-67, P.O. Box 17, H-1525 Budapest, Hungary

Received 15 November 2005; accepted 15 November 2005
Available online 20 December 2005

Dedicated to Professor Ionel Haiduc for his great contribution to Supramolecular Organometallic Chemistry.

Abstract

Three new chiral organotin(IV) carboxylates, $Me_2Sn(nap)_2$ (**1**), $\{[Me_2Sn(nap)]_2O\}_2$ (**2**) and $Me_3Sn(nap)$ (**3**) (nap = (*S*)-(+)-6-methoxy-α-methyl-2-naphthaleneaceto anion) have been synthesized. All of them have been characterized by elemental analysis, multinuclear (^1H, ^{13}C and ^{119}Sn) NMR and IR spectroscopy. The crystal structures of **1** and **2** have been determined by X-ray diffraction analysis. The bicapped tetrahedral molecules of **1** are linked by C–H···O hydrogen bonds into homochiral helices, which are also interconnected by C–H···O interactions to form an inter-helical meander-shaped network. The molecule of **2** is a parallel double helix incorporating four chiral tin centers in a $Sn_4O_{10}C_4$ ladder type molecular skeleton. The C–H···O interactions translate the molecular chirality of **2** throughout the crystal via formation of infinite ribbons. These ribbons in their turn are further cross-linked by C–H···O hydrogen bonds. The structural characterization of the complexes **1**–**3** in solution has been performed by routine multinuclear ^1H, ^{13}C and ^{119}Sn NMR as well as specialized multidimensional (^1H–^{119}Sn-gHMQC and ^1H-DOSY) experiments. The relevant $^2J_{^1H-^{119}Sn}$ and $^1J_{^{13}C-^{119}Sn}$ coupling constants have been extracted and related to molecular geometries on the basis of the literature data. The measurement of the translational diffusion constants using diffusion ordered spectroscopy allowed the estimation of the spherical hydrodynamic radii of the newly prepared structures.

Keywords: Organotin(IV) carboxylates; (*S*)-(+)-6-methoxy-α-methyl-2-naphthaleneacetic acid; Chiral; Tetraorganodistannoxane; X-ray diffraction analysis; Diffusion NMR

1. Introduction

We have been interested in the supramolecular structural chemistry of organotin(IV) complexes owing to their capacity to undergo self-assembly in solution and self-organisation in the solid state. The ability of organotin compounds to self-assemble with an increase of the coordination number of tin from four to five and six has been recognized quite early [1]. Early work in this area traces back to 1967 when Simons and Graham suggested an equilibrium between associated and unassociated forms of trimethyltin(IV) formate [1]. In 1988, Lockhart established that the di-*n*-butyltin(IV) 3-thiopropionate exists in either oligomeric or monomeric form in solution and crystallizes as a cyclic hexamer [2]. Interestingly, in spite of these early findings only few organotin(IV)-macrocycles have been created [3–18], whereas a rich structural chemistry of stannoxane and distannoxane units containing supramolecules has been emerged [19–29]. Our entry in the field of organotin supramolecular chemistry began in

* Corresponding author. Tel.: +36 1 438 1161/327; fax: +36 1 438 4141/201.
E-mail address: deak@chemres.hu (A. Deák).

0022-328X/$ - see front matter © 2005 Elsevier B.V. All rights reserved.
doi:10.1016/j.jorganchem.2005.11.038

1999, with the synthesis of trimethyltin(IV) and dimethyltin(IV) *N*-nitroso-*N*-phenylhydroxylaminates: tetrameric $[Me_3Sn(PhN_2O_2)]_4$ [30] and dimeric $[Me_2Sn(PhN_2O_2)_2]_2$ [31]. In the solid state, the tetrameric structure of $[Me_3Sn(PhN_2O_2)]_4$ incorporating a 20-membered $Sn_4O_8N_8$ inorganic ring is self-assembled by dative Sn–O bonds [30], even so the $[Me_2Sn(PhN_2O_2)_2]_2$ dimer is self-assembled by weaker stannoxanic Sn···O interactions [31]. Multinuclear multidimensional ^1H, ^{13}C and ^{119}Sn NMR data indicated that these tetrameric and dimeric supramolecules are predominantly monomeric in non-coordinating solvents at room temperature, whereas a monomer ↔ tetramer preorganisation process exists at low temperature [32]. As a result of this conformational flexibility, the tetramer is extremely reactive. We have observed that the tetramer dismutates into dimer and Me_4Sn in coordinating Lewis base solvents, such as DMSO, pyridine and methanol [32]. Interestingly, this process also took place in the solid state, and the single crystals of the tetrameric $[Me_3Sn(PhN_2O_2)]_4$ supramolecule demethylate into single crystals of $[Me_2Sn(PhN_2O_2)_2]_2$ dimer and volatile Me_4Sn [33]. This crystal-to-crystal supramolecular transformation occurs upon heating and it was accompanied by a significant change of the molecular and crystal structures [33]. Another interesting finding was that the Sn···O bonded supramolecular structure of the $[Me_2Sn(PhN_2O_2)_2]_2$ dimer can be split into monomers with nitrogen-donor bases (pyridine and 4,4′-bipyridine), and as a result 1:1 and 1:2 adducts of the monomers were formed [34]. We have identified that these organotin complexes can be connected into hydrogen bonded supramolecular structures using oxygen-donor (MeOH, EtOH) or nitrogen-donor (2,6-diamino-4-phenyl-1,3,5-triazine) coordinating ligands having the ability to participate in intermolecular hydrogen bond interactions [34]. The utility of this approach has been illustrated in the construction of hydrogen bonded dimer, infinite one-dimensional chain and double-chain [34,35].

In view of the highly variable coordination numbers and geometries of tin centers the synthesis of helical supramolecular organotin(IV) architectures, where the building units are linked via dative or hydrogen bonds represent an excellent challenge. Although, a large variety of chiral transition metal complexes have been synthesized [36,37], the class of the chiral complexes containing main group elements have been received relatively little attention by the scientific community working in this area. With such an end in mind, and owing to the fact that our research has been concerned for many years with organotin chemistry, we become interested in the preparation of enantiomerically pure complexes with potential for chiral catalysis. During the last few decades a large number of organotin(IV) carboxylates have been prepared and a multitude of structural types have been discovered [38–40]. These complexes have a tendency to self-assemble into supramolecular structures by dative Sn–O bonds (2.2–2.3 Å) and Sn···O secondary interactions (>2.5 Å) [41]. Moreover, the organotin(IV) carboxylates have been one of the most extensively studied class of anticancer compounds since it was observed that they are significantly reduce the growth rates of tumours [42–46]. We selected the (*S*)-(+)-6-methoxy-α-methyl-2-naphthaleneacetic acid, (*S*)-naproxen (Hnap), as a potent candidate for the preparation of enantiomerically pure organotin(IV)-complexes. (*S*)-Naproxen is extensively used as a nonsteroidal anti-inflammatory (NSDA) drug, which acts by inhibiting enzymes involved in the biosynthesis of prostaglandins [47]. In 1991, prior to patent expiration, (*S*)-naproxen ranked fourth in sales of optically pure pharmaceuticals [47].

2. Results and discussion

2.1. Synthesis

To prepare enantiomerically pure methyltin(IV)-naproxenates dimethyltin dichloride, dimethyltin oxide and trimethyltin chloride were allowed to react with (*S*)-naproxen or its sodium salt. The reactions gave the $Me_2Sn(nap)_2$ (**1**), $\{[Me_2Sn(nap)]_2O\}_2$ (**2**) and $Me_3Sn(nap)$ (**3**) complexes (Scheme 1). Colorless single crystals of both **1** and **2** suitable for X-ray analysis were obtained by the slow evaporation of *n*-heptane solution at room temperature.

2.2. Structural characterization in the solid state

2.2.1. $Me_2Sn(nap)_2$ (**1**)

The molecular structure of **1** is shown is Fig. 1, selected bond lengths and angles are listed in Table 1. The X-ray analysis established that the crystal contains a single enantiomer of complex **1**, and its absolute configuration was successfully determined by refining the Flack parameter [48]. When only intramolecular interactions are considered, the coordination environment of the metal center is distorted tetrahedral, in which the deprotonated carboxylate group bond to the tin center in anisobidentate fashion. The covalent, ester Sn(1)–O(1A) and Sn(1)–O(1B) bonds of 2.086(3) and 2.093(3) Å are at the short end of the range

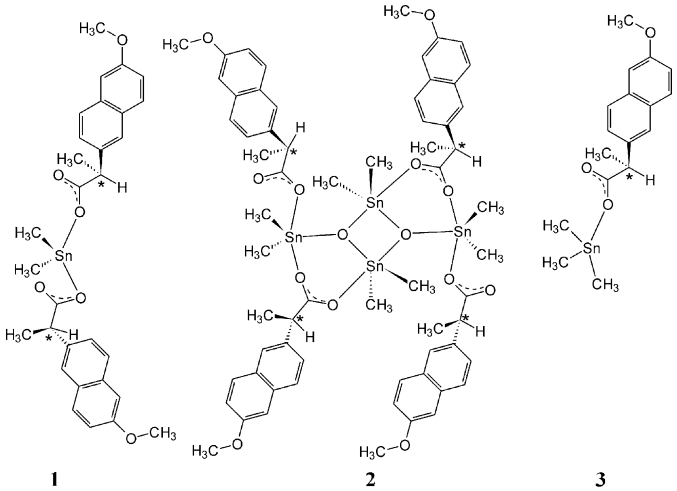

Scheme 1.

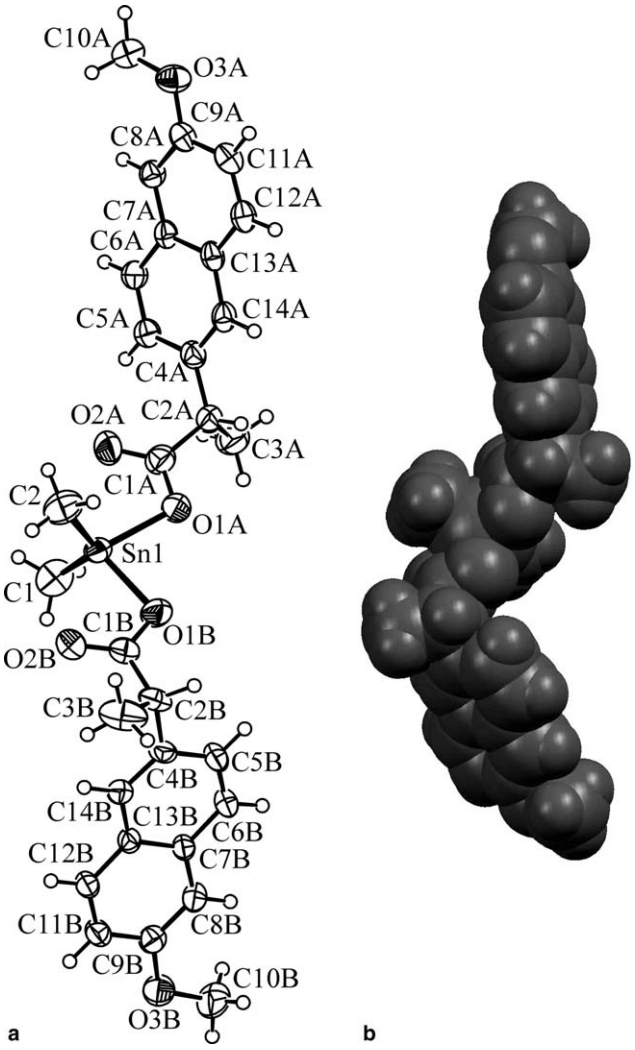

Fig. 1. (a) A view of the molecular structure of mononuclear chiral **1**. Non-hydrogen atoms are shown as 50% probability ellipsoids and hydrogen atoms are shown as open cycles. The C(2A) and C(2B) atoms are the chiral centers. (b) Space-filling plot of **1**.

Table 1
Selected bond lengths (Å) and bond angles (°) for complex **1**

Sn(1)–C(1)	2.080(6)
Sn(1)–C(2)	2.095(5)
Sn(1)–O(1A)	2.093(3)
Sn(1)–O(1B)	2.086(3)
C(1A)–O(1A)	1.264(6)
C(1A)–O(2A)	1.236(6)
C(1B)–O(1B)	1.291(6)
C(1B)–O(2B)	1.228(6)
C(1)–Sn(1)–C(2)	128.2(3)
C(1)–Sn(1)–O(1B)	111.5(2)
C(1)–Sn(1)–O(1A)	111.4(2)
O(1B)–Sn(1)–O(1A)	81.1(1)
O(1B)–Sn(1)–C(2)	107.7(2)
O(1A)–Sn(1)–C(2)	106.9(2)

found for such interactions (2.07–2.21 Å) [49]. The intramolecular special disposition of the carbonyl O(2A) and O(2B) oxygens, 2.592 and 2.597 Å, from tin is within the sum of the respective van der Waals radii (3.70 Å) [29], thus, the molecular geometry is best described as a bicapped tetrahedron [50]. These Sn···O secondary interactions could be construed as expanding the SnC_2O_2 coordination sphere about tin to SnC_2O_4. The four-membered SnO_2C_1 rings are twisted by only 6.8(2)° with respect to one another. In these rings, the strengths of the C(1A)–O(2A) and C(1B)–O(2B) bonds are comparable to that of coordinated C(1A)–O(1A) and C(1B)–O(1B) bonds (Table 1), which also confirm the existence of the Sn···O secondary interactions. Hence, there are four normal covalent bonds to tin (two Sn–C and two Sn–O), which define the tetrahedron and two Sn···O secondary interactions the capped faces. The C(1), C(2), O(1A) and O(1B) atoms of the coordination polyhedron form four normal tetrahedral O–Sn–C bond angle [ranging from 106.9(2)° to 111.5(2)°] and form two angles that show, at least in part, the effect of the capping atoms [O–Sn–O 81.1(1)° and C–Sn–C 128.2(3)°]. It should be noted here that the *cis*-bis(bidentate) complexes are inherently chiral [51], however, in our case we cannot speak about a significant helical twist in the coordination geometry, since the angle between the two planes formed by the metal and two oxygen atoms belonging to the same naproxenato ligand is −5.9(1)°.

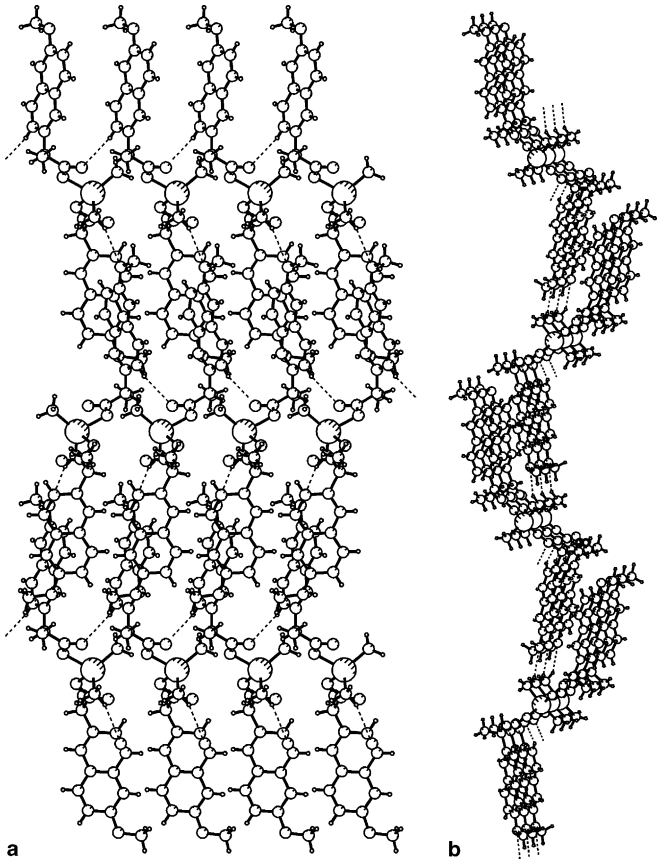

Fig. 2. (a) View illustrating the C–H···O hydrogen bonded homochiral helices **1**, which are also interconnected by C–H···O hydrogen bonds to form inter-helical network. (b) A side view of the hydrogen bonded meander-shaped network of **1**.

Table 2
Parameters of hydrogen bonding interactions in complexes **1** and **2**[a]

Complex	D–H···A	H···A (Å)	D···A (Å)	D–H···A (°)
1	C(2)–H(2G)···O(3B)[a]	2.58	3.454(7)	151
	C(5B)–H(5B)···O(2B)[b]	2.50	3.341(6)	151
2	C(2)–H(2F)···O(2C)[c]	2.48	3.391(5)	159
	C(6)–H(6B)···O(2B)[c]	2.61	3.484(5)	152
	C(3A)–H(3I)···O(3B)[d]	2.56	3.510(5)	173

[a] Symmetry codes: (a) $1-x,1/2+y,2-z$; (b) $1+x,y,z$; (c) $-1+x,-1+y,z$; (d) $-1+x,y,-1+z$.

The molecules of **1** are linked throughout C–H···O hydrogen bonding into homochiral helices (Fig. 2). This is achieved in such a way that one of the methyl hydrogen of the C(2) atom form short C–H···O hydrogen bonds (2.58 Å) with the methoxy O(3B) atom of the neighbouring molecule. In this arrangement three tin complex fragments form one helix turn with a pitch of 29.224(3) Å. Additionally, the adjacent helices are interconnected with each other by C–H···O interactions formed between the hydrogen of the naphthyl C(5B) and carboxylic O(2B) atom (Table 2). This results in the formation of an inter-helical meander-shaped network (Fig. 2(b)).

2.2.2. *{[$Me_2Sn(nap)$]$_2O$}$_2$(**2**)*

The X-ray analysis established unequivocally the absolute structure of the chiral distannoxane ladder **2** with four chiral tin atoms of the same chirality. Fig. 3 depicts the molecular structure of **2**, the selected bond lengths and angles are listed in Table 3. The central motif of this chiral ladder is a non-planar cyclic Sn_2O_2 ring, where the O(1)–Sn(3)–O(2)–Sn(4) and Sn(3)–O(2)–Sn(4)–O(1) torsion angles are 11.84° and –12.51°, respectively. The O(1) and O(2) oxygen atoms of this distannoxane ring are tridentate, as they link two endocyclic and one exocyclic tin centers. Additional links between endo- and exocyclic tin atoms are provided by two bidentate carboxylate ligands that form essentially symmetrical bridges: Sn(4)–O(2A) 2.231(3) versus Sn(1)–O(1A) 2.264(3) Å and Sn(3)–O(2D) 2.221(3) versus Sn(2)–O(1D) 2.282(3) Å. To a first approximation, the coordination geometry about each of the tin atoms is intermediate between idealized trigonal bipyramidal and square pyramidal, as revealed by the calculated τ values: 0.47, 0.49, 0.33 and 0.42 [52]. Distortions from the ideal geometries arise, in part, owing to the close intramolecular Sn···O contacts: Sn(1)···O(2B) 2.848(3), Sn(2)···O(2C) 2.867(3), Sn(3)···O(1B) 2.863(3) and Sn(4)···O(1C) 2.825(3) Å. However, these Sn···O secondary interactions are considered too long to represent significant bonding interaction, they have influence on the respective coordination geometries as seen in the expansion of the C–Sn–C angles (139.4(2)°, 134.3(2)°, 147.0(2)° and 140.4(2)°, respectively). Taking into account these weak interactions the coordination geometry of the tin centers

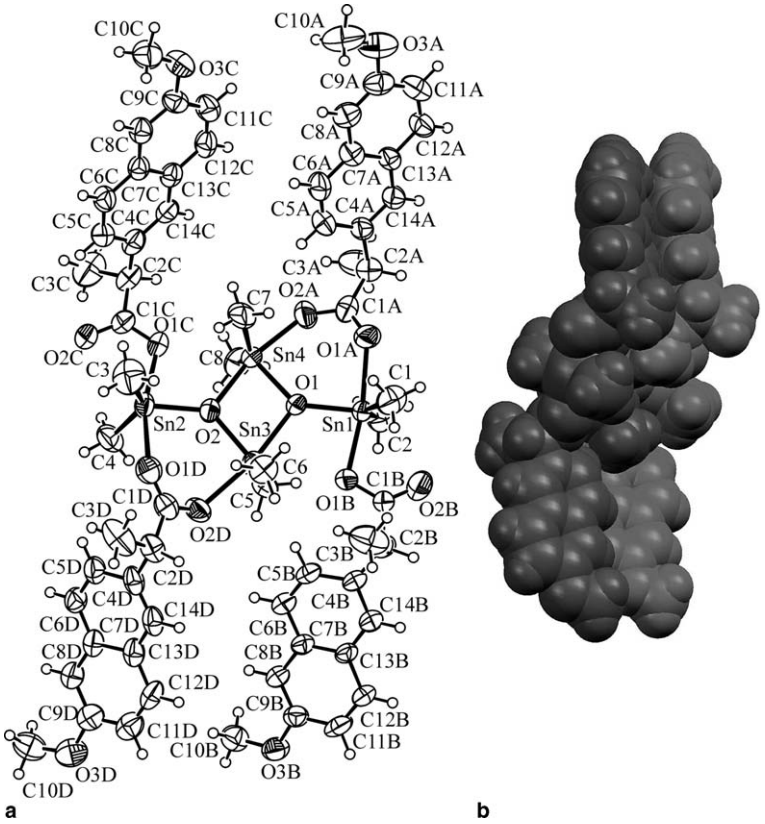

Fig. 3. (a) A view of the molecular structure of distannoxane ladder **2** with four chiral tin atoms. Non-hydrogen atoms are shown as 50% probability ellipsoids and hydrogen atoms are shown as open cycles. (b) Space-filling plot of the parallel double helix **2**.

Table 3
Selected bond lengths (Å) and bond angles (°) for complex **2**

Sn(1)–O(1)	2.010(3)	Sn(1)–C(1)	2.100(4)
Sn(1)–O(1A)	2.264(3)	Sn(1)–C(2)	2.106(4)
Sn(1)–O(1B)	2.196(3)	Sn(2)–C(3)	2.113(5)
Sn(2)–O(2)	2.017(3)	Sn(2)–C(4)	2.098(4)
Sn(2)–O(1C)	2.159(3)	Sn(3)–C(5)	2.094(4)
Sn(2)–O(1D)	2.282(3)	Sn(3)–C(6)	2.125 (4)
Sn(3)–O(2)	2.024(3)	Sn(4)–C(7)	2.117(4)
Sn(3)–O(1)	2.165(3)	Sn(4)–C(8)	2.092(5)
Sn(3)–O(2D)	2.221(3)	Sn(4)–O(2A)	2.231(3)
Sn(4)–O(1)	2.053(4)	Sn(4)–O(2)	2.154(3)
C(1A)–O(1A)	1.229(5)	C(1B)–O(1B)	1.292(5)
C(1A)–O(2A)	1.279(5)	C(1B)–O(2B)	1.225(6)
C(1C)–O(1C)	1.295(5)	C(1D)–O(1D)	1.253(5)
C(1C)–O(2C)	1.256(5)	C(1D)–O(2D)	1.289(6)
O(1)–Sn(1)–C(1)	112.3(2)	O(1)–Sn(1)–O(1A)	88.5(1)
O(1)–Sn(1)–C(2)	107.1(1)	O(1)–Sn(1)–O(1B)	81.9(1)
C(1)–Sn(1)–C(2)	139.4(2)	C(1)–Sn(1)–O(1B)	92.8(2)
O(1)–Sn(1)–O(1A)	88.5(1)	O(1B)–Sn(1)–O(1A)	167.5(1)
C(2)–Sn(1)–O(1A)	88.3(1)	C(1)–Sn(1)–O(1A)	83.3(1)
O(2)–Sn(2)–O(1C)	78.7(1)	O(2)–Sn(2)–O(1D)	85.5(1)
O(1C)–Sn(2)–O(1D)	165.8(1)	C(4)–Sn(2)–C(3)	134.3(2)
O(2)–Sn(2)–C(3)	112.2(2)	O(2)–Sn(2)–C(4)	112.1(1)
C(4)–Sn(2)–O(1D)	88.1(2)	C(3)–Sn(2)–O(1D)	84.6(2)
C(4)–Sn(2)–O(1C)	101.2(2)	C(3)–Sn(2)–O(1C)	97.7(2)
O(2)–Sn(3)–O(1)	77.0(1)	O(2)–Sn(3)–O(2D)	90.3(1)
O(1)–Sn(3)–O(2D)	166.6(1)	C(5)–Sn(3)–C(6)	147.0(2)
O(2)–Sn(3)–C(5)	107.2(1)	O(2)–Sn(3)–C(6)	105.5(2)
O(2)–Sn(3)–C(4)	105.4(2)	C(5)–Sn(3)–O(1)	93.4(1)
C(5)–Sn(3)–O(2D)	86.3(1)	C(6)–Sn(3)–O(2D)	89.6(2)
O(1)–Sn(4)–O(2)	76.6(1)	O(1)–Sn(4)–O(2A)	89.9(1)
O(2)–Sn(4)–O(2A)	165.8(1)	C(7)–Sn(4)–C(8)	140.4(2)
O(1)–Sn(4)–C(7)	108.4(2)	O(1)–Sn(4)–C(8)	110.6(1)
C(7)–Sn(4)–O(2)	97.9(1)	C(8)–Sn(4)–O(2)	97.2(1)
C(7)–Sn(4)–O(2A)	90.5(1)	C(8)–Sn(4)–O(2A)	83.3(2)

can be best described as skew-trapezoidal-bipyramidal [53]. A quantitative measure of the helical twist around the exocyclic tin centres is given by the sequence of the dihedral angles formed between the coordinated carboxylate oxygen atoms. Thus, the O(2A)–O(1A)–O(1B)–O(2B) and O(2D)–O(1D)–O(1C)–O(2C) dihedral angles are 143.72° and 138.41°, and are clearly indicative of a helical twist. Moreover, these two individual helices are rotated by 11.6° with respect to one another, in such a way that the overall molecule is a parallel double helix (Fig. 3(b)). In this conformation, the ladder type $Sn_4O_{10}C_4$ molecular skeleton (the r.m.s. deviation from the best plane is 0.33 Å) is formed by three four-membered Sn_2O_2 and two SnO_2C_1 as well as two six-membered $Sn_2O_3C_1$ fused rings (Fig. 4). It should be noted here that according to the Q, θ and φ puckering parameters (Table 4) the six-membered Sn(1)–O(1)–Sn(4)–O(2A)–C(1A)–O(1A) and Sn(2)–O(1D)–C(1D)–O(2D)–Sn(3)–O(2) rings show chiral screw-boat and a twist-boat conformations, which are twisted by 23.9(1)° with respect to one another. To the best of our knowledge only one report has appeared so far for a double ladder structure containing eight different chiral tin centers [54].

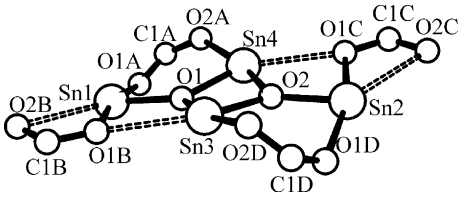

Fig. 4. A view of the $Sn_4O_{10}C_4$ molecular skeleton incorporating three four-membered Sn_2O_2 and two SnO_2C_1 as well as two six-membered $Sn_2O_3C_1$ fused rings, showing the helical twist in the structure of complex **2**.

Table 4
Puckering parameters of the two six-membered $Sn_2O_3C_1$ rings of the molecular skeleton of complex **2**

Ring	Q (Å)	θ (°)	φ (°)
Sn(1)–O(1A)–C(1A)–O(2A)–Sn(4)–O(2)	0.797(2)	91.4(2)	25.3(2)
Sn(1)–O(1)–Sn(4)–O(2A)–C(1A)–O(1A)	0.564(4)	101.4(3)	154.6(3)

Complementary intermolecular C–H···O hydrogen bonding was observed between the C(2)–H(2F) methyl hydrogen and the carboxylic O(2C) atom as well as C(6)–H(6B) methyl hydrogen and the carboxylic O(2C) atom (Table 2). These C–H···O interactions translates the molecular chirality of **2** throughout the crystal via formation of infinite ribbons (Fig. 5). Moreover, the C(3A)–H(3I) methyl hydrogen of the chiral C(2A) atom and the methoxy O(2C) atom of the neighbouring ribbons are also engaged in C–H···O hydrogen bonding. As a result, the C–H···O hydrogen bonded Z-shaped ribbons are further cross-linked via C–H···O hydrogen bonds to their respective neighbours (Fig. 5).

2.3. Structural characterization of *1–3* in the liquid phase by NMR spectroscopy

Compounds **1–3** have been characterized by solution ^1H, ^{13}C and ^{119}Sn NMR spectroscopy. The Me–Sn–Me angles were calculated from the $^1J_{^{13}C-^{119}Sn}$ and $^2J_{^1H-^{119}Sn}$ scalar coupling constants (Table 5) using the validated method of Lockhart et al. [55,56]. We aimed to verify whether the chiral moiety adjacent to the carboxylate ligand influences the spectroscopic properties of the prepared compounds in comparison to the literature data of achiral carboxylate derivatives [57].

For complexes **1** and **3** no major deviances from reference compounds (e.g., acetates, benzoates) have been found [57–59]. The relevant spectral data ($^1J_{^{13}C-^{119}Sn}$, $^2J_{^1H-^{119}Sn}$, $\delta_{^{119}Sn}$) of compound **1** is in line with the well known distorted octahedral (O_h) geometry provided, that in this case the carboxylates are anisobidendate and the central tin is hexacoordinated. The ca. 133° for the Me–Sn–Me angle however, is also indicative of the equilibrium contribution of a distorted tetrahedron in which the carboxylates are temporarily monodendate. When **1** was dissolved in pyridine-d_5, both of its characteristic J-coupling contants have increased ($^1J_{^{13}C-^{119}Sn}/^2J_{^1H-^{119}Sn} = 1064/108.3$ Hz) corresponding to significantly higher 170/179°

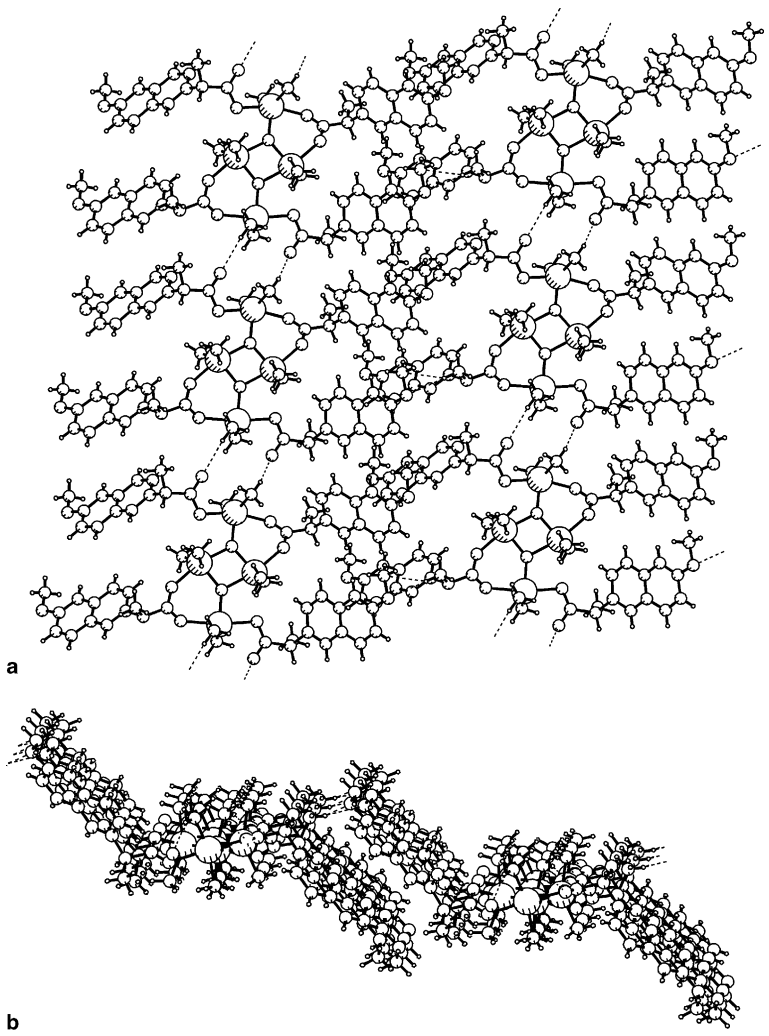

Fig. 5. (a) View illustrating the C–H···O hydrogen bonded infinite ribbons of **2**, and the C–H···O hydrogen bonded cross-link between them. (b) A side view of the cross-linked hydrogen bonded *Z*-shaped ribbons of **2**.

Table 5
Values of the Me–Sn–Me bond angles (°) from X-ray data and calculated from $^{2}J(^{119}Sn–^{1}H)$ [55] and $^{1}J(^{119}Sn–^{13}C)$ [56] coupling data measured in solution

Compound	Me–Sn–Me		
	X-ray	$^{2}J(^{119}Sn–^{1}H)$	$^{1}J(^{119}Sn–^{13}C)$
1	128.2(3)	133.2	133.4
$\mathbf{2}_{endo}$	147.0(2)	143.0	143.1
	140.4(2)		
$\mathbf{2}_{exo}$	139.4(2)	139.4	145.8
	134.3(2)		
3	–	111.0	111.4

Me–Sn–Me angles. This phenomenon has been recently attributed to solvent coordination leading to a heptacoordinated tin center [32]. However, our attempt to determine the equilibrium binding constant for the monopyridine solvate of **1** has failed, because of the hydrolytic instability of the system in the presence of the base.

Fig. 6. shows the ^{1}H NMR spectrum of **1** in $CDCl_3$ after pyridine-h_5 was added to the system. The sharp resonances

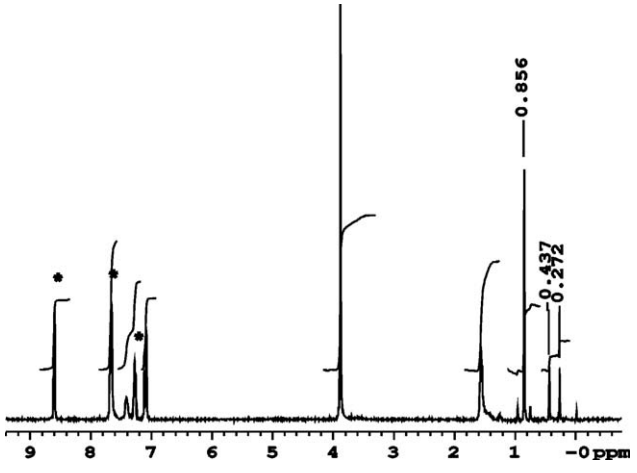

Fig. 6. ^{1}H NMR spectrum (400 MHz) of **1** in the presence of pyridine (denoted by ∗) in $CDCl_3$ at 25 °C.

upfield (at 0.44 and 0.27 ppm) to the methyl singlet of the main component were tentatively assigned to the exo- and endocyclic methyl groups of the corresponding

tetraorganodistannoxane **2**. Formation of this latter from **1** has been verified by two independent ways: (A) using state-of-the-art NMR methods and (B) via direct chemical synthesis of **2**.

Fig. 7. shows the ^{1}H DOSY (diffusion ordered spectroscopy) [60,61] experiment recorded for **1** in $CDCl_3$/pyridine-h_5 where formation of **2** became evident. The crosspeaks assigned to the components are well separated along the diffusion (vertical) axis. The diffusion constants (dotted line) has been determined on the basis of proton assignments using the non-overlapping resonances only. The endo- and exocyclic methyls of **2** gave correlation peaks to the same diffusion constant ($D = 4.8 \times 10^{-10}$ m^2/s) indicating that they are both part of the same molecular entity. Since the spherical hydrodynamic radius r is inversely proportional to the diffusion constant D according to the Stokes–Einstein relation [62],

$$D = \frac{k_B T}{6\pi\eta r} \tag{1}$$

the hydrolysis product **2** have proved to fit in a larger radius sphere ($r_2 = 8.5$ Å) than **1** (with $r_1 = 6.1$ Å) (k_B is the Boltzmann-constant, T is absolute temperature, η is viscosity). We note that as a consequence of the free rotation around the C–C bonds [e.g. C(1A)–C(2A) and C(2A)–C(4A)] the molecules – when dissolved – are actually less ellipsoidal and more spherical in shape. The aromatic protons of **1** and **2** are in complete overlap giving rise to weight averaged diffusion crosspeaks, dominated by the diffusion characteristics of the main component. A further proof of the structure in case of the in situ formed **2** has been obtained by the interpretation of the ^{1}H–^{119}Sn-HMQC experiment (Fig. 8) [63–66]. The appearance of the pair of doublet crosspeaks at ($\delta_{^{119}Sn}$: −176.2 and −183.8 ppm) is the characteristic of a bis-dicarboxylatotetraorganodistannoxane, in which both the exo- and the endocyclic tin atoms are pentacoordinated. The same information is available from the almost identical ^2J values (89 and 91 Hz). The two pairs of exo- and endocyclic tin atoms are linked by a bidentate, bridging carboxylate ligand while the remaining carboxylate groups behave as monodentate ligands with exocyclic tin atoms. Apparently, the $Sn_4O_{10}C_4$ skeleton of **2** is maintained in solution, while the ligand part of the system does not show any conformational preference.

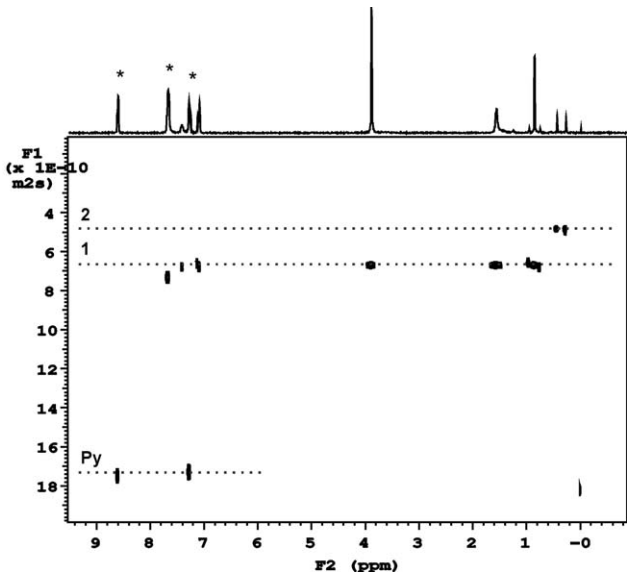

Fig. 7. ^{1}H DOSY NMR of **1** in the presence of pyridine (denoted by ∗) verifying the formation of **2** in $CDCl_3$ at 25 °C. The horizontal scale represents the ^{1}H dimension, whereas the vertical scale shows the diffusion scale (m^2/s).

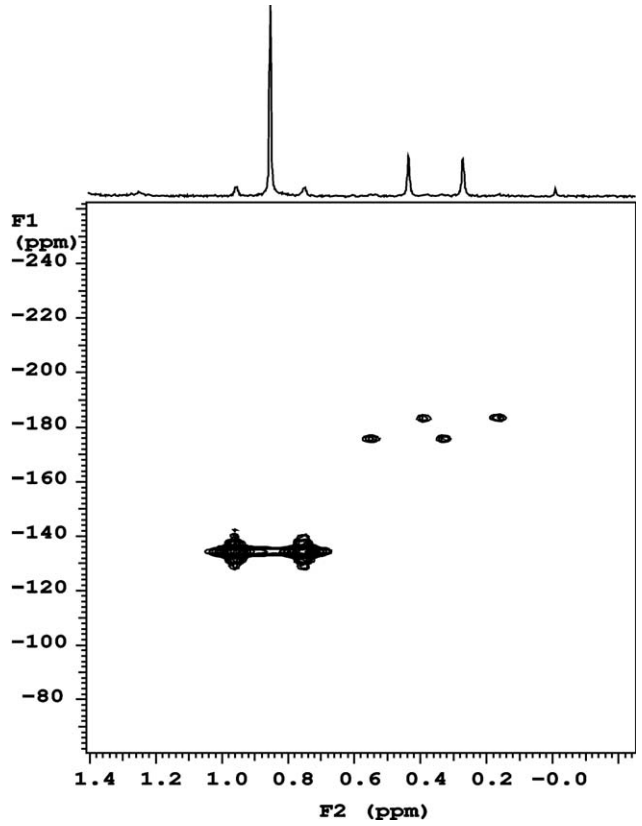

Fig. 8. ^{1}H–^{119}Sn-gHMQC spectrum of **1** recorded in the presence of pyridine ($CDCl_3$, 25 °C). The horizontal and vertical scales represent the ^{1}H and ^{119}Sn dimensions, respectively.

The single ^{119}Sn resonance of compound **3** at 135.5 ppm, as well as the 111° Me–Sn–Me angle indicates a distorted tetrahedron (T_h) with tin coordination number 4. Accordingly, **3** is monomeric in solution and the single carboxylate is predominantly monodendate [59].

3. Experimental

3.1. Materials

Trimethyltin(IV) chloride, dimethyltin(IV) dichloride and (*S*)-(+)-6-methoxy-α-methyl-2-naphthaleneacetic acid were purchased from Aldrich as pure compounds and used as received. Dimethyltin(IV) oxide was prepared from

dimethyltin(IV) dichloride by following a literature method [67]. The preparation and purification of the complexes were carried out in the open air or in a dry atmosphere. FT-IR spectra were recorded with a NICOLET 160SX FT-IR spectrometer.

3.2. Synthesis of complex $Me_2Sn(nap)_2$ (1)

The aqueous solution of Me_2SnCl_2 (0.22 g, 1 mmol) was added to an aqueous solution containing (*S*)-naproxen (0.46 g, 2 mmol) and Na_2CO_3 (0.116 g, 1 mmol). Complex **1** promptly precipitated. After stirring for half an hour at room temperature, the white precipitate was filtered off. Recrystallization from *n*-heptane gave the product as colorless prismatic crystals. M.p. > 155 °C. Yields, 0.535 g (0.881 mmol, 87.7%). Anal. Calc. for $C_{30}H_{32}O_6Sn$: C, 59.3; H, 5.3. Found: C, 59.2; H, 5.2%. IR (KBr, cm^{-1}): $\nu(COO)_{as}$ 1631sh, 1605vs; $\nu(COO)_s$ 1384s; ν(Sn–C) 576w, 541m; ν(Sn–O) 480m. ^1H NMR (399.89 MHz, $CDCl_3$): δ 0.88 (s, $^2J(^{117}Sn/^{119}Sn–^1H) = 79.1/81.8$ Hz, 3H, CH_3); 1.57 (d, $J = 7.2$ Hz, 3H, CH_3), 3.90 (q, $J = 7.2$ Hz, 1H, CH), 3.91 (s, 3H, CH_3), 7.09–7.16 (m, 2H, CH), 7.41 (dd, $J = 8.4$, 1.8 Hz, 1H, CH), 7.65–7.72 (m, 3H, CH). ^{13}C NMR (100.56 MHz, $CDCl_3$): δ 4.1 (s, $^1J(^{117}Sn/^{119}Sn–^{13}C) = 618/646$ Hz, CH_3), 18.9 (s, CH_3), 45.3 (s, CH_2), 55.3 (s, CH_3), 105.6 (s, CH), 118.9 (s, CH), 125.9 (s, CH), 126.1 (s, CH), 127.1 (s, CH), 128.9 (s, C), 129.3 (s, CH), 133.7 (s, C), 135.7 (s, C), 157.6 (s, C), 184.7 (s, C). ^{119}Sn NMR (149.08 MHz, $CDCl_3$): δ −118.2 ppm.

3.3. Synthesis of $\{[Me_2Sn(nap)]_2O\}_2$ (2)

To a solution of Me_2SnO (0.33 g, 2 mmol) in toluene/ethanol (3:1) was added a solution of (*S*)-naproxen (0.46 g, 2 mmol) in ethanol. The reaction mixture was refluxed for 4 h with azeotropic removal of water via Dean-Stark trap. The reaction mixture was concentrated, cooled to yield the white solid of **2**. Recrystallization from *n*-heptane gave the product as colorless blocky crystals. M.p. > 155 °C. Yields, 0.72 g (0.466 mmol, 93.5%). Anal. Calc. for $C_{64}H_{76}O_{14}Sn_4$: C, 49.8; H, 5.0. Found: C, 49.9; H, 5.2%. IR (KBr, cm^{-1}): $\nu(COO)_{as}$ 1671m, 1647m, 1605s, 1550vs; $\nu(COO)_s$ 1454s, 1294s; ν(Sn–O–Sn) 657m, 640m, ν(Sn–O) 546m; ν(Sn–O) 503m. ^1H NMR (399.89 MHz, $CDCl_3$): δ 0.28 (s, br, $^2J(^{117}Sn/^{119}Sn–^1H) = 88.7$ Hz, 3 H, CH_3), 0.45 (s, $^2J(^{117}Sn/^{119}Sn–^1H) = 86.3$ Hz, 3 H, CH_3), 1.44 (d, $J = 7.2$ Hz, 3H, CH_3), 3.57 (q, $J = 7.2$ Hz, 1H, CH), 3.89 (s, 3H, CH_3), 7.07–7.13 (m, 2H, CH), 7.31 (d, $J = 8.4$ Hz, 1H, CH), 7.57 (s, 1H, CH), 7.61–7.67 (m, 2H, CH). ^{13}C NMR (100.56 MHz, $CDCl_3$): δ 6.0 (s, $^1J(^{117}Sn/^{119}Sn–^{13}C) = 721/756$ Hz, CH_3), 8.4 (s, $^1J(^{117}Sn/^{119}Sn–^{13}C) = 756/787$ Hz, CH_3), 19.0 (s, CH_3), 47.3 (s, CH_2), 55.3 (s, CH_3), 105.6 (s, CH), 118.8 (s, CH), 125.9 (s, CH), 126.3 (s, CH), 127.0 (s, CH), 128.9 (s, C), 129.2 (s, CH), 133.5 (s, C), 137.0 (s, C), 157.4 (s, C), 180.6 (s, C). ^{119}Sn NMR (149.08 MHz, $CDCl_3$): δ −175.8 [$^2J(^{119}Sn–^{117}Sn/^{119}Sn) = 97$ Hz] and −183.4 [broad, $^2J(^{119}Sn–^{117}Sn/^{119}Sn)$ unresolved].

3.4. Synthesis of $Me_3Sn(nap)$ (3)

The aqueous solution of Me_3SnCl (0.2 g, 1 mmol) was added to an aqueous solution containing (*S*)-naproxen (0.23 g, 1 mmol) and Na_2CO_3 (0.053 g, 0.5 mmol). Complex **3** promptly precipitated. After stirring for half an hour at room temperature, the white precipitate was filtered off. Recrystallization from *n*-heptane gave the product as colorless acicular crystals. M.p. 141–142 °C. Yields, 0.27 g (0.687 mmol, 69.2%). Anal. Calc. for $C_{17}H_{22}O_3Sn$: C, 51.9; H, 5.6. Found: C, 51.8; H, 5.8%. IR (KBr, cm^{-1}): $\nu(COO)_{as}$ 1631s, 1605vs, 1572s, 1556sh; $\nu(C{=}O)_s$ 1391ms, 1345ms; ν(Sn–C) 551ms; ν(Sn–O) 477m. ^1H NMR (399.89 MHz, $CDCl_3$): δ 0.50 (s, $^2J(^{117}Sn/^{119}Sn–^1H) = 56.0/58.0$ Hz, 9H, CH_3), 1.55 (d, $J = 7.2$ Hz, 3H, CH_3), 3.85 (q, $J = 7.2$ Hz, 1H, CH), 3.91 (s, 3H, CH_3), 7.10–7.15 (m, 2H, CH), 7.43 (dd, $J = 8.4$, 1.8 Hz, 1H, CH), 7.65–7.72 (m, 3H, CH). ^{13}C NMR (100.56 MHz, $CDCl_3$): δ −2.5 (s, $^1J(^{117}Sn/^{119}Sn–^{13}C) = 378/395$ Hz, CH_3), 19.4 (s, CH_3), 46.0 (s, CH_2), 55.3 (s, CH_3), 105.6 (s, CH), 118.7 (s, CH), 125.8 (s, CH), 126.4 (s, CH), 126.9 (s, CH), 129.0 (s, C), 129.3 (s, CH), 133.5 (s, C), 137.1 (s, C), 157.4 (s, C), 179.9 (s, C). ^{119}Sn NMR (149.08 MHz, $CDCl_3$): δ +135.5 ppm.

3.5. Physical measurements

3.5.1. X-ray crystallography

Crystal data and refinement parameters are summarised in Table 6. Intensity data for **1** were collected on an Enraf-Nonius CAD-4 diffractometer with graphite monochromated Mo Kα radiation ($\lambda = 0.71073$ Å) using the ω-2θ scan technique. Three standard reflections were monitored every hour; these remained constant within experimental error. Intensity data for **2** were collected on a Rigaku R-AXIS RAPID image plate diffractometer (λ(Mo Kα radiation) = 0.71070 Å) at 93 ± 2 K. The system was equipped with an X-stream cryo-cooler for low temperature studies. The structures were solved by direct methods (SHELXS-97) and refined by full-matrix least-squares (SHELXL-97) [68]. All non hydrogen atoms were refined anisotropically in F^2 mode. Hydrogen atomic positions were generated from assumed geometries. The riding model was applied for the hydrogen atoms.

3.5.2. NMR experiments

The NMR spectra were recorded on a 400 MHz (for ^1H) Varian INOVA spectrometer equipped with a Varian 5 mm $^1H–^{19}F/\{^{15}N–^{13}P\}$ Z-gradient indirect detection probe and a direct detection Varian $^{15}N–^{13}P/\{^1H–^{19}F\}$ switchable broadband probe. ^1H and ^{13}C chemical shifts are referenced to the residual solvent signals, whereas ^{119}Sn shifts are given relative to the external Me_4Sn (0.00 ppm) signal.

Table 6
Crystal data and structure refinement parameters for complexes **1** and **2**

	1	**2**
Empirical formula	$C_{30}H_{32}O_6Sn$	$C_{64}H_{76}O_{14}Sn_4$
Formula mass	607.25	1544.01
Crystal size (mm)	$0.15 \times 0.40 \times 0.50$	$0.58 \times 0.58 \times 0.59$
Temperature (°C)	22	−180
Crystal system	Monoclinic	Triclinic
Space group	$P2_1$	$P\bar{1}$
θ Range for data collection (°)	$2.47 \leqslant \theta \leqslant 34.24$	$3.15 \leqslant \theta \leqslant 27.48$
a (Å)	5.662(1)	9.8706(17)
b (Å)	29.224(3)	10.1917(19)
c (Å)	8.259(1)	16.751(3)
α (°)	90	90.039(8)
β (°)	90.70(3)	100.370(8)
γ (°)	90	106.316(8)
V (Å^3)	1366.5(3)	1588.5(5)
Z	2	1
μ (mm^{-1})	0.976	1.617
Index ranges (°)	$-8 \leqslant h \leqslant 8$; $-46 \leqslant k \leqslant 46$; $-13 \leqslant l \leqslant 13$	$-12 \leqslant h \leqslant 12$; $-13 \leqslant k \leqslant 13$; $-21 \leqslant l \leqslant 21$
No. of reflections collected	12564	73767
No. of independent reflections/R_{int}	11297/0.028	14372/0.038
No. of observed reflections [$I > 2\sigma(I)$]	7169	14034
No. of parameters	340	755
Goodness-of-fit on F^2	0.99	1.21
R_1 (observed data)	0.0461	0.0301
wR_2 (all data)	0.1345	0.0799
Flack parameter	0.02(2)	−0.006(13)

99.95% perdeuterated solvents were purchased from Merck Gmbh, Germany. Room temperature ^{119}Sn chemical shift data were partially obtained from ^{1}H–^{119}Sn-gHMQC experiments. The $^1J(^{119}Sn–^{13}C)$ coupling constants were determined from the ^{119}Sn satellites seen in $F1$ traces of the gradient enhanced ^{1}H–^{13}C-HSQC experiments (2.7 Hz digital resolution). The DOSY experiment was carried out in a 2 mm capillary placed in a 3 mm tube ($CDCl_3$ matched) at 25 °C to minimize convection effects. Performa I gradient amplifier was used. The gradient strength was calibrated by using 5 w/w% sucrose in D_2O at 25 °C ($D = 5.22\ E^{-10}$ m^2/s). The *bipolar pulse-pair stimulated echo* pulse-sequence was used for acquiring diffusion data with 50 ms diffusion delay, 16 squared increments for gradient levels and 16 transients. The Varian DOSY package was used for the processing. Chloroform viscosity $\eta = 5.42$ mPa · s was used for the calculation of the hydrodynamic radii at 25 °C.

Acknowledgements

We thank NKFP 1/A/005/2004 MediChem2 for financial support. We are thankful to Mrs. Judit Vinkler for providing the FT-IR spectra.

Appendix A. Supplementary data

Crystallographic data (excluding structure factors) for the structures reported in this paper have been deposited with the Cambridge Crystallographic Data Center as supplementary publication Nos. CCDC-286648 (**1**) and CCDC-286649 (**2**). Copies of the data can be obtained free of charge on application to CCDC, 12 Union Road, Cambridge CB2 1EZ, UK [Fax: int. code +44(1223)336 033; E-mail: deposit@ccdc.cam.ac.uk]. Supplementary data associated with this article can be found, in the online version, at doi:10.1016/j.jorganchem.2005.11.038.

References

[1] P.B. Simons, W.A. Graham, J. Organomet. Chem. 8 (1967) 479.
[2] T.P. Lockhart, Organometallics 7 (1988) 1438.
[3] C. Pettinari, F. Marchetti, R. Pettinari, D. Martini, A. Drozdov, S. Troyanov, J. Chem. Soc., Dalton Trans. (2001) 1790.
[4] C. Pettinari, F. Marchetti, R. Pettinari, A. Cingolani, A. Drozdov, S. Troyanov, J. Chem. Soc., Dalton Trans. (2002) 188.
[5] C. Ma, F. Li, D. Wang, H. Yin, J. Organomet. Chem. 667 (2003) 5.
[6] C. Ma, Q. Jiang, R. Zhang, D. Wang, J. Chem. Soc., Dalton Trans. (2003) 2975.
[7] C. Ma, J. Sun, J. Chem. Soc., Dalton Trans. (2004) 1785.
[8] C. Ma, Y. Han, R. Zhang, D. Wang, Dalton Trans. (2004) 1832.
[9] R. García-Zarracino, J. Ramos-Quiñones, H. Höpfl, Inorg. Chem. 42 (2003) 3835.
[10] R. García-Zarracino, H. Höpfl, J. Am. Chem. Soc. 127 (2005) 3120.
[11] V. Chandrasekhar, V. Baskar, A. Steiner, S. Zacchini, Organometallics 23 (2004) 1390.
[12] M.G. Newton, I. Haiduc, R.B. King, C. Silvestru, Chem. Commun. (1993) 1229.
[13] R. Cea-Olivares, O. Jiménez-Sandoval, G. Espinoza-Pérez, C. Silvestru, J. Organomet. Chem. 484 (1994) 33.
[14] M. Gielen, A. El Khloufi, M. Biesemans, F. Kayser, R. Willem, B. Mahieu, D. Maes, J.N. Lisgarten, L. Wyns, A. Moreira, T.K. Chattopadhay, R.A. Palmer, Organometallics 13 (1994) 2849.
[15] K.C. Molloy, F.A.K. Nasser, C.L. Barnes, D. van der Helm, J.J. Zuckerman, Inorg. Chem. 21 (1982) 960.
[16] J.G. Masters, F.A.K. Nasser, M.B. Hossain, A.P. Hagen, D. van der Helm, J.J. Zuckerman, J. Organomet. Chem. 385 (1990) 39.
[17] S.W. Ng, V.G.K. Das, G. Pelizzi, F. Vitali, Heteroatom Chem. 1 (1990) 433.
[18] G. Prabusankar, R. Murugavel, Organometallics 23 (2004) 5644.
[19] R. Holmes, Acc. Chem. Res. 22 (1989) 190.
[20] G. Prabusankar, R. Murugavel, Organometallics 23 (2004) 5644.
[21] V. Chandrasekhar, R.O. Day, R.R. Holmes, Inorg. Chem. 24 (1985) 1970.
[22] V. Chandrasekhar, C.G. Schmid, S.D. Burton, J.M. Holmes, R.O. Day, R.R. Holmes, Inorg. Chem. 26 (1987) 1050.
[23] R.R. Holmes, C.G. Scmid, V. Chandrasekhar, R.O. Day, J.M. Holmes, J. Am. Chem. Soc. 109 (1987) 1408.
[24] K.C. Kumara Swamy, M.A. Said, S. Nagabrahmanandachari, D.M. Poojary, A. Clearfield, J. Chem. Soc., Dalton Trans. (1998) 1645.
[25] R.O. Day, V. Chandrasekhar, K.C. Kumara Swamy, J.M. Holmes, D. Burton, R.R. Holmes, Inorg. Chem. 27 (1988) 2887.
[26] V. Chandrasekhar, S. Negendran, S. Bansal, M.A. Kozee, D.R. Powell, Angew. Chem., Int. Ed. 39 (2000) 1833.
[27] M. Mehring, G. Gabriele, S. Hadijikakou, M. Schürmann, D. Dakternieks, K. Jurkschat, Chem. Commun. (2002) 834.
[28] M. Mehring, M. Schürmann, H. Reuter, D. Dakternieks, K. Jurkschat, Angew. Chem., Int. Ed. 36 (1997) 1112.
[29] V. Chandrasekhar, V. Baskar, K. Gopal, J.J. Vittal, Organometallics 24 (2005) 4926.

[30] A. Deák, I. Haiduc, L. Párkányi, M. Venter, A. Kálmán, Eur. J. Inorg. Chem. (1999) 1593.
[31] A. Deák, M. Venter, A. Kálmán, L. Párkányi, L. Radics, I. Haiduc, Eur. J. Inorg. Chem. (2000) 127.
[32] G. Tárkányi, A. Deák, Organometallics 24 (2005) 3784.
[33] A. Deák, G. Tárkányi, Chem. Commun. (2005) 4074.
[34] A. Deák, L. Radics, A. Kálmán, L. Párkányi, I. Haiduc, Eur. J. Inorg. Chem. (2001) 2849.
[35] A. Deák, Sz. Kárpáti, Gy. Vankó, A. Kálmán, I. Haiduc, Inorg. Chim. Acta 358 (2005) 1012.
[36] U. Knof, A. von Zelewsky, Angew. Chem., Int. Ed. 38 (1999) 302.
[37] A. von Zelewsky, O. Mamula, J. Chem. Soc., Dalton Trans. (2000) 219.
[38] R. Okawara, D.E. Webster, E.G. Rochow, J. Am. Chem. Soc. 82 (1960) 3287.
[39] V. Chandrasekhar, S. Nagendran, V. Baskar, Coord. Chem. Rev. 235 (2002) 1.
[40] M. Gielen, M. Biesemans, D. de Vos, R. Willem, J. Inorg. Biochem. 79 (2000) 139.
[41] I. Haiduc, F.T. Edelman, Supramolecular Organometallic Chemistry, Wiley-VCH Verlag GmbH, Germany, 1999, pp. 154.
[42] I. Haiduc, C. Silvestru, Organometallics in Cancer Chemotherapy Main Group Metal Compounds, vol. I, CRC Press, Boca Raton, FL, 1989, pp. 129.
[43] M. Gielen, P. Lelieveld, D. de Vos, R. Willem, in: M. Gielen (Ed.), Metal Based Antitumour Drug, vol. 2, Freund Publication, Tel Aviv, 1992, pp. 29.
[44] M. Gielen, E.R.T. Tiekink, in: M. Gielen (Ed.), Metallotherapeutic Drug and Metal-Based Diagnostic Agents, Wiley, Chichester, 2005, p. 421 (Chapter 22: ^{50}Sn Tin Compounds and their Therapeutic Potential).
[45] R. Di Stefano, M. Scoppelliti, C. Pellerito, G. Casella, T. Fiore, G.C. Stocco, R. Vitturi, M. Colomba, L. Ronconi, I.D. Sciacca, L. Pellerito, J. Inorg. Biochem. 98 (2004) 534.
[46] L. Pellerito, L. Nagy, Coord. Chem. Rev. 224 (2002) 111.
[47] P.J. Harington, E. Lodewijk, Organic Process Research and Development 1 (1997) 72.
[48] H.D. Flack, Acta Crystallogr. A39 (1983) 876.
[49] K.C. Molloy, T.G. Purcell, K. Quill, I.W. Nowell, J. Organomet. Chem. 267 (1984) 237.
[50] S.P. Narula, S.K. Bharadwaj, Y. Sharda, R.O. Day, L. Howe, R.R. Holmes, Organometallics 11 (1992) 2206.
[51] M. Brorson, T. Damhus, C.E. Schäffer, Inorg. Chem. 22 (1983) 1569.
[52] A.W. Addison, T.N. Rao, J. Reedijk, J. van Rijn, G.C. Verschoor, J. Chem. Soc., Dalton Trans. (1984) 1349.
[53] W.F. Howard Jr., R.W. Crecely, W.H. Nelson, Inorg. Chem. 24 (1985) 2204.
[54] D. Dakternieks, A. Duthie, B. Zobel, K. Jurkschat, M. Schürmann, E.R.T. Tiekink, Organometallics 21 (2002) 647.
[55] T.P. Lockhart, W.F. Manders, Inorg. Chem. 25 (1986) 892.
[56] T.P. Lockhart, F. Davidson, Organometallics 6 (1987) 2471.
[57] T.P. Lockhart, W.F. Manders, E.M. Holt, J. Am. Chem. Soc. 108 (1986) 6611.
[58] T.P. Lockhart, J.C. Calabrese, F. Davidson, Organometallics 6 (1987) 2779.
[59] M. Nádvorník, J. Holeček, K. Handlíio, A. Lyčka, J. Organomet. Chem. 315 (1986) 299.
[60] K.F. Morris, C.S. Johnson Jr., J. Am. Chem. Soc. 114 (1992) 3139.
[61] C.S. Johnson Jr., Prog. Nucl. Magn. Reson. 34 (1999) 203.
[62] J.T. Edward, J. Chem. Educ. 47 (1970) 261.
[63] F. Ribot, C. Sanchez, A. Meddour, M. Gielen, E.R.T. Tiekink, M. Biesemans, R. Willem, J. Organomet. Chem. 552 (1998) 177.
[64] F. Kaiser, M. Biesemans, M. Boualam, E.R.T. Tiekink, A.E. Khloufi, J. Meunier-Piret, A. Bouhdid, K. Jurkschat, M. Gielen, R. Willem, Organometallics 13 (1994) 1098.
[65] R. Willem, A. Bouhdid, A. Meddour, C. Camacho-Camacho, F. Mercier, M. Gielen, M. Biesemans, F. Ribot, C. Sanchez, E.R.T. Tiekink, Organometallics 16 (1997) 4377.
[66] J.C. Martins, M. Biesemans, R. Willem, Progr. Nucl. Magn. Reson. 36 (2000) 271.
[67] R.K. Ingham, S.D. Rosenberg, H. Gilman, Chem. Rev. 60 (1960) 459.
[68] G.M. Sheldrick, SHELXS97 – Program for Crystal Structure Determination and SHELXL97 – Program for the Refinement of Crystal Structures, University of Göttingen, Germany, 1997.